

OPTICAL PROPERTIES OF SPRAYED TIN OXIDE FILMS

By

*Dr. Majid M. Shukur**

*Dr. Fadhel M. Hasson**

*Mr. Mosaad M. Ali**

**Materials Engineering College- Babylon University*

Abstract

This research is intended to study the preparation of heat mirror by spray pyrolysis method. Un-doped tin oxide (SnO_2) and doped with 0.09%, 0.9%, and 9%, titanium dioxide heat mirror films were deposited on pre-cleaned substrates. The microstructure characterizations were carried out by x-ray diffraction technique. The optical properties were obtained by UV-Visible spectrophotometer. The un-doped samples have displayed average transmittance value of 73% in the visible region. Whereas, the doped samples of 0.09 and 0.9 mol% TiO_2 show a good reflectance values of 76% and 80% respectively in the wavelength of 2700 nm.

Keywords: tin oxide, thin films, spray pyrolysis, optical properties.

المستخلص

تم في هذه الدراسة تحضير أغشية نقية من ثاني اوكسيد القصدير و أخرى مشوبة بثاني اوكسيد التيتانيوم و بتراكيز (0.09 ، 0.9 ، 9) % و مرسبة على أسطح قاعدة من الزجاج و بطريقة الرش الكيماوي الحراري. تم معرفة خصائص هذه الأغشية و بنياتها من خلال الأشعة السينية الحادة. كما تم الحصول على خصائصها البصرية باستخدام مطياف الأشعة فوق البنفسجية- المرئية، حيث أعطت الأغشية النقية نفاذية للأشعة المرئية بحدود 73%، في حين كانت الانعكاسية للأغشية المشوبة بتراكيز (0.09 و 0.9) % ثاني اوكسيد التيتانيوم 76% و 80% على التوالي و عند الطول الموجي 2700 نانومتر.

الكلمات الرئيسية: اوكسيد القصدير ، الأغشية الرقيقة ، الرش الحراري ، الخواص البصرية.

1. Introduction

Tin oxide is used as heat mirror coating for windows. The main characteristics of heat mirror are high solar transmittance and high infrared reflectance (Hirunlabh, 1998). Thin films of tin oxides are well known as transparent conducting oxides (Ghafoor, 1986). It will be interesting to know that under a certain conditions, they are transparent to visible and reflected infrared radiations. So, these properties make them suitable for various applications. It has been experimentally found that in solar heat collectors, the emittance of heat to the environment of SnO_2 mirror is a minimum. As a result of this, thin films can also be applied on car-windows to prevent ice deposition of cloudiness nights (Manifacier and Murcia, 1977; Gobel and Schierbaum, 1991; Kim and Laitinen, 1975; and Chaturvedi, 1999). Thin films of tin oxide have another advantage that they can be produced in an inexpensive manner on large surfaces.

A variety of methods have been used to deposit tin oxide films such as sol-gel (Horvath, 2005) metal organic (Chaturvedi, 1999) chemical vapour deposition (CVD) (Viguie and Spitz, 1975) sputtering (Stamate, 2000) and spray pyrolysis. Among these techniques, spray pyrolysis is well suited for preparation of pure and doped tin oxides thin films. This method has many advantages such as simple and inexpensive experimental arrangement, ease of adding materials, reproducibility, high growth rate, mass production, and capability for uniform large area coating. These advantages are desirable for industrial selective surface and solar cells applications (Ghfoor, 1986 ; Al-Maamoory, 1990 ; Hirunlabh, 1998 ; Al-Mermadhi, 2003 ; and Lampert, 1992) . In this paper, we present preparation thin films of SnO₂ which doped by various concentrations of TiO₂ to deposit on glass substrate by pyrolysis method. These films will be investigated to a visible transmittance and reflected infrared radiations.

2. Theory Background

2.1 Lattice parameters

Lattice parameters of SnO₂ thin films were determined by comparing the peak positions of the XRD patterns of the film with that is appeared for SnO₂ in the joint committee on powder diffraction standards (JCPDS) . It is known that the structural lattice of SnO₂ phase has a tetragonal structure. The lattice constants of SnO₂ thin film are calculated by the relation:

$$1/d^2 = (h^2 + k^2)/a^2 + l^2/c^2 \quad (1)$$

Where:

- d = The distance between adjacent planes in the set (hkl),
- (hkl) = Miller's indices,
- a, and c = lattice constants.

2.2 Crystallite – size determination

To perform crystallite – size measurements by X – ray line broadening, a diffraction peaks (110) and (002) for the thin film of SnO₂ are carefully scanned by a diffractometer. The observed peak widths, usually measured at half width – maximum intensity in angular degrees. Then corrected for instrumental and K α – doublet broadening. The main crystallite dimension D is then related to the corrected line breadths by the Scherrer equation: (Rau, 1962)

$$D = K\lambda / \beta \cos\theta \quad (2)$$

Where: K = crystallite – shape constant equal to 0.94

λ = X – ray wavelength

β = corrected line breadth

θ = Bragg angle

This crystallite size should be considered as an average distance between lattice imperfection rather than the size of polycrystalline grains.

2.3 Dislocation density and microstrain

The growth mechanism of thin films involving dislocation is important from the subject point of view. In thin crystalline films, the presence of defects not only serve to disrupt the geometric regularity of the lattice on a microscopic level, but significantly influence on many film properties such as chemical reactivity, electrical conduction, and mechanical behaviour (Meyers and Chawly, 1999 ; Kittel, 1996 ; and Dekker, 1971). The dislocation density (δ) can be evaluated from the crystallite size (D) by the relation: (Karumajaran, 2002)

$$\delta = n/D^2 \quad (3)$$

Where (n) is a factor, when it equals unity, it gives a minimum dislocation density. The origin of microstrain is related to the lattice misfit, which in turn depends upon the deposition condition. The microstrain (ϵ_s) which is developing in the SnO₂ thin films can be calculated from the relation:

$$\epsilon_s = (\lambda/D \cdot \cos\theta - \beta) (1/\tan\theta) \quad (4)$$

2.4 Structural analysis

X – ray diffraction peaks of SnO₂ thin films are indexed on the bases of a tetragonal unit cell. The lattice constants of a – axis and c – axis and calculated interplanar spacing are calculated by the plane – spacing equation $1/d^2 = (h^2+k^2)/a^2 + l^2/c^2$. Volume of the unit cell is also calculated by using the formula $V = a^2 * c$. Calculated density of SnO₂ thin films was obtained by using the formula:

$$\rho_{cal.} = (M_w * Z * 1.66)/V \quad (5)$$

Where:

ρ_{cal} = calculated density (g/cm³)

M_w = molecular weight of SnO₂ (mol/g)

Z = number of SnO₂ in unit cell

1.66 = reciprocal Avogadro number

V = volume of unit cell (A^o)³

3. Experimental Techniques and Procedures

A schematic diagram of locally-made experimental setup for spray pyrolysis is shown in Figure 1.

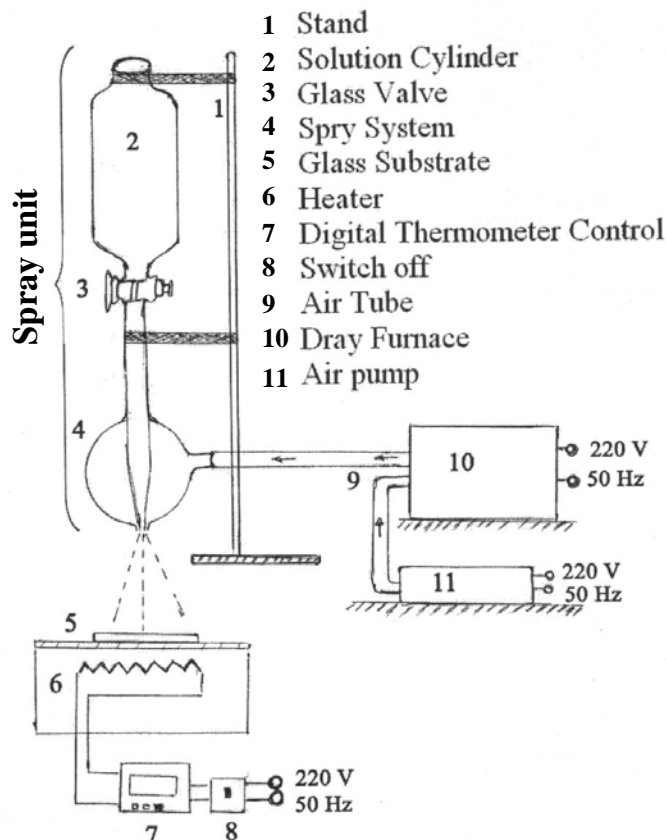


Figure 1: Schematic diagram of experimental setup.

The head of spray unit consists of capillary glass tube joint from an upper end with solution cylinder by a glass valve and from a lower end with gradually reduced diameter to form the spray nozzle and surrounds by spherical glass which is joined with air compressing pump. The air is compressed through a network of pipes inside the dried oven. This step is intended to prevent crash of the substrate as a result of thermal shock. The substrate heater, basically resistively heat wire, is covered with a stainless plate on which the substrate is placed. The temperature is measured using a thermocouple; which is controlled by a digital controller. The coating was achieved on (75×25×1) mm slide glass. The glass substrate temperature was fixed at 450°C to obtain thin film of thickness about 0.12 μm.

High purity powder of SnO₂ was dissolved in 10 ml of concentrated hydrochloric acid and then mixed by a magnetic stirrer of 15 minutes. As a result, the transparent solution is diluted with distilled water to get a stock solution. For TiO₂ doping, high purity powder of TiO₂ was dissolved in 10 ml of concentrated hydrochloric acid and then heating at 50°C for 1 hour. The resulting solution is diluted with distilled water. Accordingly, the spraying solution is contained titania concentrations of 0.0%, 0.09%, 0.9%, and 9%,. The deposition rate was 2.25 ml/min, and the normalized distance between the spray nozzle and glass substrate was 30-33 cm. Whereas the spray time was ≈ 30 second with interval time of ≈ 60 second.

Simadzu-6000 X-ray diffractometer with a nickel filter using monochromatized CuKα radiation at 40 Kv and 30 mA was used throughout to detect the crystalline structure of the films. The films were scanned at 2° (2θ) per min. and the scan range was 20° 2θ to 60° 2θ. The intensity was recorded with a chart speed of 25 mm/min.

The transmittance and absorbance of the films were measured in the 190-110 nm region by means of Shimadzu UV-1600 series double-beams spectrophotometer, and reflectance was measured in the 300-2700 nm by means of lambda 9 spectrophotometer.

4. Results and Discussion

Table 1 represents X- ray diffraction data for pure SnO₂ thin film in comparison with that of doped SnO₂ thin film.

Table 1 X- ray data for doped SnO₂ thin film.

Doped (SnO ₂)				Pure (SnO ₂)			
No.	2θ°	d(A°)	I/I _o	2θ°	d(A°)	I/I _o	(hkl)
1	26.9588	3.34855	100	26.5306	3.35701	100	110
2	33.9019	2.64206	14	33.8125	2.6488	58	101
3	37.0792	2.36128	80	37.8518	2.37494	29	200
4	51.8216	1.76282	25	51.6687	1.76767	46	211
5	54.7304	1.6758	8	54.6063	1.67932	10	220
6	57.82	1.5934	6	57.82	1.5934	6	002
System: Tetragonal a = 4.7326A° c = 3.13903A° V = 70.3082(A°) ³ Z = 2 M _w = 144.319 ρ _{cal.} = 6.81484 g/cc				System: Tetragonal a = 4.74908 A° c = 3.18896 A° V = 71.923 (A°) ³ Z = 2 M _w = 150.69 ρ _{cal.} = 6.9559 g/cc			

Table 2 explains the corrected line breadth (β), mean crystallite dimension (D), dislocation density (δ), and the microstrain (ϵ_s) for pure SnO₂ thin film.

Table 2 Structural analysis data for pure SnO₂ thin film.

Sample	2 θ°	d(A $^\circ$)	(hkl)	B	β	D(A $^\circ$)	$\delta \cdot 10^{-4}$ (A $^\circ$) ⁻²	ϵ_s *10 ⁻³	Axes
SnO ₂ pure	26.5306	3.35701	110	0.5	0.4915	173.445	0.3324	2.325	a-axis
	57.8200	1.5934	002	2.5	2.4770	38.266	6.8290	5.0	c-axis

B = width of diffraction curve at half intensity (1/2I_{max}).

Table 3 explains the structural analysis data for the doped SnO₂ thin film.

Table 3 Structural analysis data for doped SnO₂ thin film.

Sample	2 θ°	d(A $^\circ$)	(hkl)	B	β	D(A $^\circ$)	$\delta \cdot 10^{-4}$ (A $^\circ$) ⁻²	ϵ_s *10 ⁻³	Axes
Doped SnO ₂	26.5988	3.34855	110	0.25	0.24	355.253	0.0790	1.135	a-axis
	57.8200	1.5934	002	1.5	1.481	64.001	2.4410	2.985	c-axis

Figure 2 shows the proper peaks planes of pure and doped SnO₂ thin films.

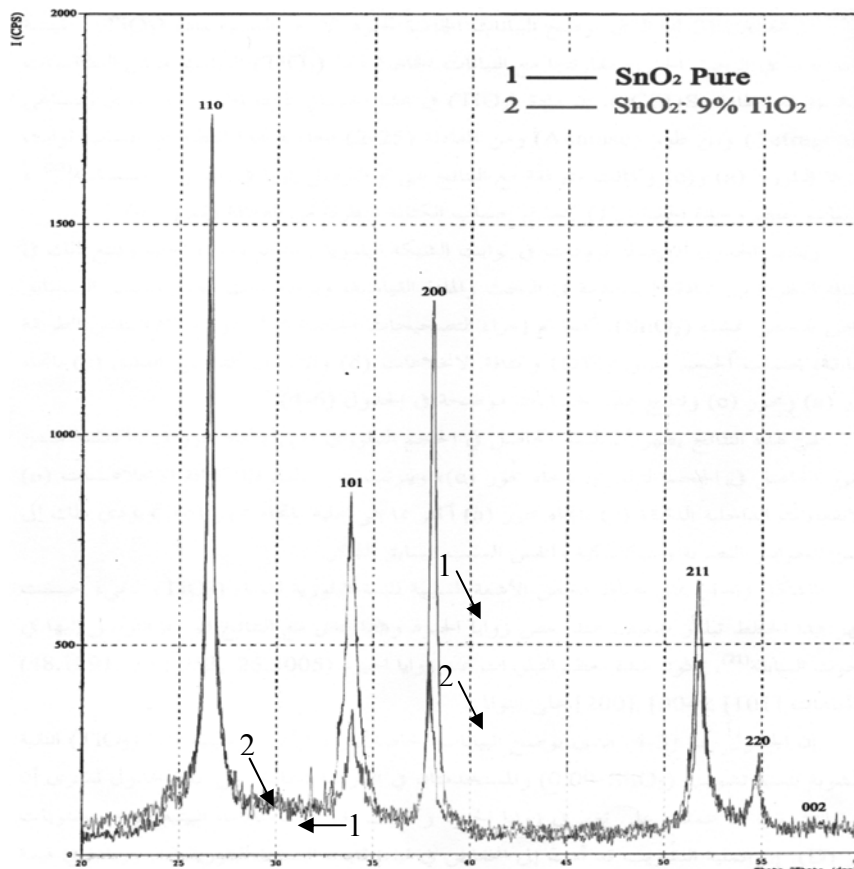


Figure (2): X-ray diffraction for pure and doped SnO₂ thin film

According to this figure and tables (2 & 3), it has been observed that there are a preferable orientation in crystal direction of [110] for doped thin film in comparison with that of pure thin film. The little reducing of both a and c axes for unit cell of doped thin film causes a notable increasing in crystallite size dimension in both axes. Consequently, the volume unit cell of doped thin film has been reduced as a result of substitution between primary large tin atoms ($r = 0.69 \text{ \AA}$) and secondary relatively small titanium atoms ($r = 0.61 \text{ \AA}$) (Kingery et al., 1975). The atomic substitution of doped thin film gave rise to points defects in crystalline lattice and also led to shrink the crystalline lattice of doped thin film (Sn,Ti)O₂.

The crystallite size (D) of the doped thin film is found to increase with doping process. As a result of this, the dislocation density (δ) and microstrain (ϵ_s) make clear a decreasing trend with doping process, and hence the doped thin film has less imperfections (Karumajaran, 2002).

4.1 Transmittance

Figure 3 shows the transmittance of (190-1100) nm wavelength for pure and doped thin films. The average transmittance in the visible region for pure SnO₂ thin film and doped SnO₂ thin films with (0.09%, 0.9%, 9%) TiO₂ are approximately 71.5%, 75%, 75.5%, and 52% respectively. The lower visible transmittance of 9 mol % TiO₂ thin film (52%) is created by the energy levels of the band gap. Consequently, a degradation in absorption edge is occurred and hence the absorption wavelength is increasing. On the other hand, the upper visible transmittance was found at 0.9 mol % TiO₂ thin film which is considered the best result for domestic applications.

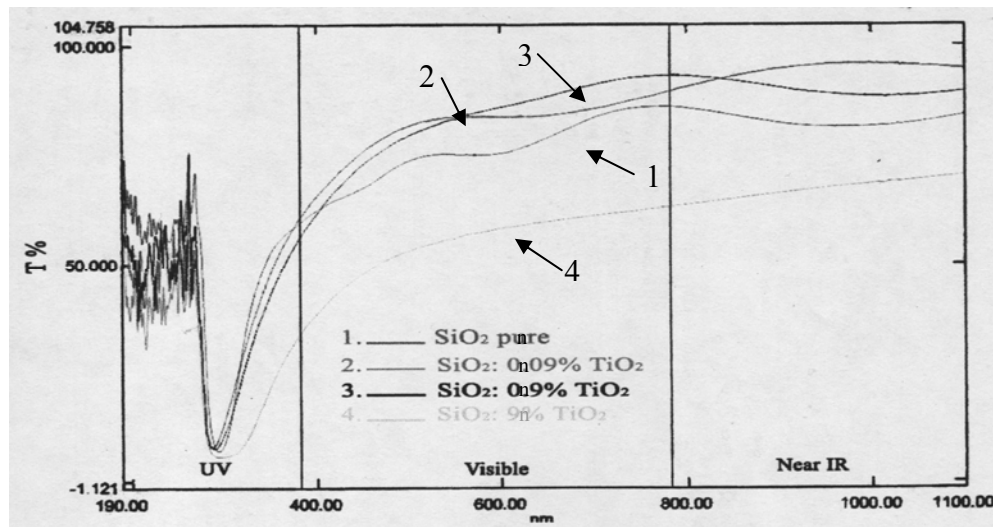
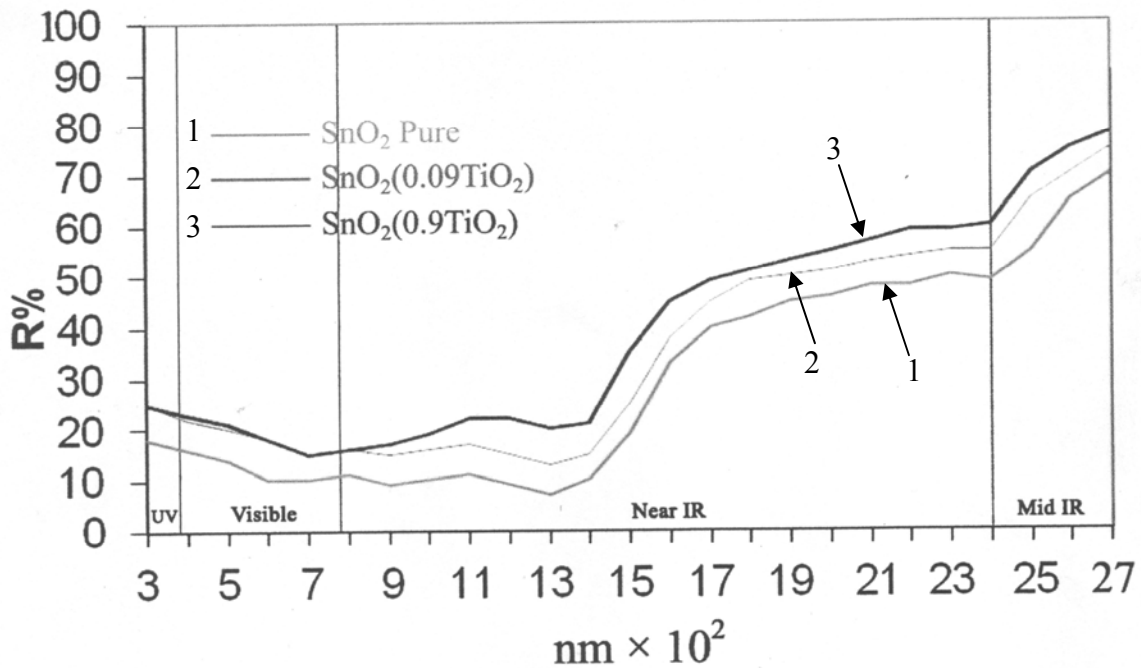


Figure (3): Transmittance of SnO₂ thin film

4.2 Reflectance

Figure 4 shows the reflectance range of (300-2700) nm of pure and doped SnO₂ thin films. The average reflectance in the IR region of pure and doped with 0.09 and 0.9 mol are approximately reached to 70%, 75%. And 80% respectively at wavelength of 2700 nm. It has been observed that the doped thin film with 0.9 mol TiO₂ has the best reflectance for IR radiation. This result comes from the view of the fact that the lower dislocation density and microstrain cause to reduce grain boundaries in the structure of doped thin film.

Figure (4): Reflectance of SnO₂ thin film

5. Conclusions

Based on our data for the preparation of thin films of favoured quality of glass window, the conclusions is that:

1. Doped SnO₂ thin films with different concentrations of TiO₂ are polycrystalline with tetragonal structure.
2. The crystalline lattices of the doped SnO₂ thin film have reduced their dimensions, and this led to increase the crystallite size which directly decreasing of dislocation density and microstrain.
3. Doped SnO₂ thin film with 0.9 mol TiO₂ has a good transmittance for visible radiations and well reflectance for IR radiations.

6. References

- Al-Maamoory, M.M., 1990**, Study of structural and electroptical for ZnO thin films by X-ray diffraction. M.Sc. thesis, University of Basrah [in Arabic].
- Al-Mermadhi, R.A., 2003**, Preparation of selective surfaces to reflect thermal radiations. M.Sc. thesis, University of Babylon [in Arabic].
- Chaturvedi, A., 1999**, Response of oxygen plasma treated thin film tin oxide sensor array for LPG, CCl₄, Co, C₃H₇OH. J. Microelectro., V. 30.
- Dekker, A.J., 1971**, Solid state physics.
- Ghafoor, W.S., 1986**, Study the properties of PbS and SnO₂ thin films by chemical pyrolysis. M.Sc. thesis, University of Basrah [in Arabic].
- Gobel, W. and Schierbaum, K.D., 1991**, Transport and sensors properties of nanostructure antimony-doped tin oxide films, Sensor. Actuat. B-Chem., V. 26, No. 27.
- Hirunlabh, J., 1998**, Development of spray pyrolysis coating process for tin oxide film heat mirrors, J. Sci. technol., V.3, No. 2, pp (10-20).

- Horvath, E., 2005**, Investigation of SnO₂ thin film evaluation by hermoanalytical and spectroscopics methods, Appl. Surface Sci, V.242, pp (13-20).
- Karumajaran, B., 2001**, Influence of thermal annealing on the composition and structural parameters of D.C. reactive magnetron sputtering titanium dioxide thin films, Cryst. Res. Technol., V. 37, No. 12, pp (1285-1292), India.
- Kim, H. and Laitinen, H.A., 1975**, Microstructure of SnO₂ conductive film prepared by pyrohydrolytic decomposition on to glass substrate, J.Am.Ceram. Soc., V.58, p 23.
- Kingery, W.D., Bowen, H.K., and Uhlmann, D.R., 1975**, Introduction to ceramics, 2nd edition, John Wiley, New York.
- Kittle, Ch., 1996**, Introduction to solid state physics, John Wiley & Sons, USA.
- Lampert, C.M., 1992**, Optical properties of transparent conductive thin films for solar energy utilization, Material chemistry, V.21, pp (612-616).
- Manifacier, C., and DE Murcia, M., 1977**, optical properties of Zn – Ti films, Thin Solid Film, V.41, pp (127-135).
- Meyers, M.A., and Chawly, K.K., 1999**, Mechanical behaviour of materials, USA, Prentice-Hall, Inc., p 675.
- Rau, R.C., 1962**, **Advances in X-ray analysis, V.5, plenum press, New York, pp (104-116).**
- Stamate, N., 2000**, Dielectric of TiO₂ thin films deposited by D.C. Magnetron Sputtering System, Thin Solid Films, V.372, pp (246-249).
- Viguie, J.C. and Spitz, J., 1975**, Chemical Vapour Deposition (CVD) at low temperature, J. Electrochem. Soc., V.122, pp (585-588).